Characterization of the 32 μs isomer in ^{189}Pb as a shears-mode bandhead

G. D. Dracoulis,[*] G. J. Lane, T. Kibédi, and P. Nieminen[†]

Department of Nuclear Physics, RSPhysSE, Australian National University, Canberra ACT 0200, Australia

(Received 22 December 2008; published 5 March 2009)

Internal conversion coefficients have been measured for transitions following the decay of the 32 μs isomer in the neutron-deficient isotope ^{189}Pb. The main branch at 337 keV to the $25/2^+$ excited state is shown to be of $E3$ multipolarity with a strength of about 24 W.u. This, together with multipolarity assignments to other branches, leads to a spin and parity assignment of $K^\pi = 31/2^-$ for the 2435-keV state. This also defines that state as the isomer, rather than the lifetime being due to feeding from a higher lying $33/2^+$ isomeric state as had been proposed previously. The isomer is suggested to arise from the partially aligned coupling of the 11^- two-proton configuration with the $i_{13/2}$ neutron hole. The low-lying nature of the $31/2^-$ multiplet member is attributed to the change in quasiparticle character of the $i_{13/2}$ neutron configuration as the neutron shell is depleted.

The neutron-deficient Pb isotopes exhibit a rich variety of spherical and deformed nuclear structures. These include the multiparticle states formed through proton-core excitation and occupation of $h_{9/2}$, $i_{13/2}$, and $f_{7/2}$ proton orbitals above the $Z = 82$ closed shell, and combinations of these with neutron-hole excitations. Excitations such as the 11^- state from the $\pi s_{1/2}^{-2} h_{9/2} i_{13/2}$ configuration have been identified in the even-even isotopes, from ^{196}Pb down to the neutron-deficient isotope ^{188}Pb (see Refs. [1–3] for systematics). Although nominally spherical, a moderate oblate deformation for this state is implied from calculations and static moment measurements. The argument has also been made that the $11^- \rightarrow 8^+$ $E3$ transitions (known for $A = 190$–196) are more enhanced than expected because the oblate deformation causes hybridization of the 8^+ state wave function [4,5]. The presence of isomers and collective bands in ^{188}Pb and ^{190}Pb is evidence for a triple shape coexistence (spherical, oblate, and prolate) [1,3] and the existence of three 0^+ states in the more neutron-deficient case ^{186}Pb has similar implications [6]. The role of intruder states and shape coexistence in Hg, Pb, and Po isotopes and experimental advances in studying very neutron deficient cases have been recently reviewed [7].

Yet one more aspect of structure in this region has been the identification of so-called shears bands as extensively documented [8–10]. These quasicollective structures arise (in the simplest cases) from the coupling of the 11^- two-proton excitation to the $i_{13/2}$ neutron hole (or holes), resulting in angular momentum vectors that are partially aligned at the bandhead and subsequently become more parallel as higher spin states are formed. Fully aligned coupling (parallel) in the case of a single $i_{13/2}$ neutron would give $J_{max} = 35/2^-$ but a perpendicular coupling is favored by the repulsive proton/neutron-hole residual interaction. As a consequence, the "bandhead" spin should increase as the neutron shell is more depleted since the character of the neutron excitation

becomes more particle-like and less hole-like in moving away from the upper part of the shell. Such coupled configurations are expected to have a similar oblate deformation to that of the 11^- core [11], although this has not been proven experimentally.

In the case of Pb isotopes near mid-shell, excited states have been identified in ^{191}Pb [12] and ^{189}Pb [13] and in the even-even neighbors [1,3]. These include two relatively long-lived isomers ($J^\pi = 11^-$, $\tau = 11$ μs and $J^\pi = 12^+$, $\tau = 36$ μs) in ^{190}Pb and a 32 μs isomer in ^{189}Pb. The latter was tentatively assigned to a $33/2^+$ state expected from the seniority-three, $\nu i_{13/2}^{-n}$ configuration with a retarded decay caused by mid-shell seniority cancellation [13]. This assignment was tentative in that in the attribution it was assumed that an unobserved low-energy $E2$ transition fed an excited state at 2435 keV, which itself had a tentative $29/2^+$ assignment. Firmer assignment of spins and parities was not possible in the absence of information such as internal conversion coefficients. Such measurements had been attempted but had not been successful because of the low production cross section [13]. In general, Pb isotopes with $A < 190$ become increasingly more difficult to study because of the competition from fission and the resultant contaminant γ-ray fluxes and reduced fusion-evaporation cross sections.

The present results are the first obtained with a new recoil spectrometer, under development for the study of the γ-ray and electron spectroscopy of isomeric states in heavy nuclei where fission competition is a limitation. The spectrometer [14] uses SOLITAIRE, a compact superconducting solenoidal fusion product separator [15] on the beam axis to transport fusion-evaporation residues to an approximate focus, about 1.9 m downstream from the target. The solenoid is filled with low-pressure gas (usually a mixture of helium and nitrogen) so that the recoiling ions effectively sample the average equilibrium charge state. Because of the differences in magnetic rigidity, most beam-like particles and fission products can be intercepted in small-diameter baffles on the beam axis, whereas the majority of long-lived fusion-evaporation products ($\tau \geqslant$ 300 ns), which follow helical orbits at larger angles, survive to the rear. The residues are implanted at shallow depth at the focal plane, where they are viewed by an upstream

————————
[*]Corresponding author: george.dracoulis@anu.edu.au

[†]Present address: Department of Physics, University of Jyväskylä, P. O. Box 35, FI-40014 Jyväskylä, Finland.

(annular) array of six cooled Si(Li) electron detectors inside the vacuum chamber and γ-ray detectors, located downstream and outside the vacuum chamber. In this arrangement, a large solid angle is provided for electron detection in the backward hemisphere. Note that the electron peak detection efficiency is approximately constant in the range ~200 keV to 1 MeV. In the current preliminary configuration, a single large-volume Ge detector was used, together with a single LEPS detector for detection of γ rays.

The experiment used the ^{164}Er(^{29}Si, $4n$)^{189}Pb reaction with beams provided by the ANU 14UD Pelletron accelerator. The beam was chopped with macroscopic pulse lengths of 33 μs separated by intervals of 170 μs. The target was a self-supporting foil of thickness 700 μg/cm^2, resulting in scattered recoils emerging from the rear of the target with energies of about 20 MeV. (The target is within the gas volume.) Depending on the gas pressure and magnetic field, the efficiency for transporting residues to the active detection area with such an asymmetric reaction is estimated to be about 50% [14]. All γ rays and electrons were measured with respect to a clock register, relative to the beam pulsing. The conditions were chosen to give reasonable population of the known isomer, and also to have a sufficiently long out-of-beam period to facilitate subtraction of long-lived activities via a difference between short and long time regions. (A similar technique was used, for example, in Ref. [4].)

Complementary measurements were also carried out with the same target (backed in this case with a gold foil to stop recoils) and time conditions, and the CAESAR γ-ray array, to determine the optimum energy for production of ^{189}Pb, given the uncertainty in predicting cross sections when fission is a strong channel. The energy chosen (145 MeV) was significantly higher than the effective energy in the earlier measurement [13].

Figure 1 shows the simultaneously measured γ-ray and electron spectra obtained by taking a delayed time region with
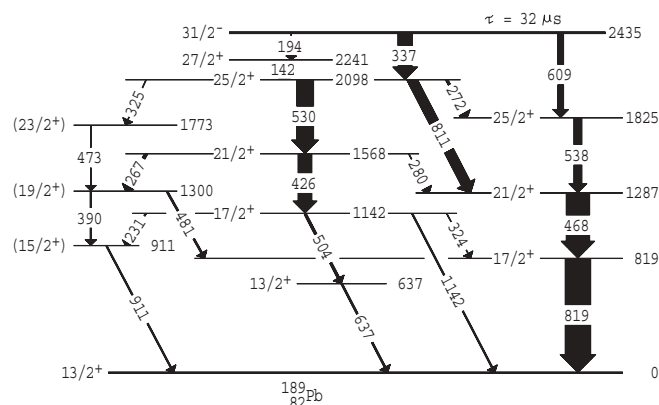
FIG. 2. Level scheme of ^{189}Pb adapted from Ref. [13] with spin assignments from the present study.

a width of about 85 μs, with a subsequent, contiguous time region subtracted. The level scheme adapted from Ref. [13] is shown in Fig. 2. The main γ-ray transitions following the isomeric decay in ^{189}Pb are clear. Population of the comparably long-lived isomers in ^{190}Pb, arising mainly from the $5n$-evaporation reaction on the ^{166}Er isotopic component in the target, was also observed. Measurements optimized for ^{190}Pb with ^{28}Si beams and an ^{166}Er target were also carried out, allowing correction for the majority of that contamination to be made.

Several features stand out in comparing the γ-ray and electron spectra. These include the strong conversion of the 337-keV transition, the main γ-ray branch from the 2435-keV excited state (Fig. 2). It shows a distinctive $E3$ signature, with both high absolute conversion and an L line that is more intense than the K line. Further, close examination of the line shapes shows that the L (and M) lines are complex, consistent with the significant energy differences and population among the L subshells in Pb. The most intense electron lines observed can be attributed to the 194-keV transition from the 2435-keV state whose weak γ-ray branch is not observed with significant intensity in Fig. 1 but is known from the previous work [13] and confirmed in our complementary γ-ray studies.

Its large conversion coefficient and K/L ratio leads to an $M2$ assignment, as shown in Table I. Conversion from the high-energy $E2$ transitions, such as the 819-keV line, is weak, but a significant electron line corresponding to K conversion of the 637-keV $13/2^+ \rightarrow 13/2^+$ transition is observed. It is known from both total conversion [13] and direct measurement [17] to have a large $E0$ component.

By combining the previous results [13] with the conversion coefficients given in Table I, it is possible to confirm assignments to the main states lower in the scheme and to assign $J^\pi = 31/2^-$ to the 2435-keV state. One consistency check on the new assignment is the intensity balance through the weak 194/142 keV γ-ray cascade to the $25/2_2^+$ state. The delayed γ-ray intensities are given as $I_\gamma(142) = 35(5)$ and $I_\gamma(194) = 22(5)$ in Ref. [13]. Taking $(1 + \alpha_T) = 4.45$ for the 142-keV $M1$ transition and $(1 + \alpha_T) = 8.03$ for a 194-keV $M2$ transition leads to $I_{\text{tot}}(142) = 156(22)$, to be compared with $I_{\text{tot}}(194) = 176(40)$. These match within the errors; it
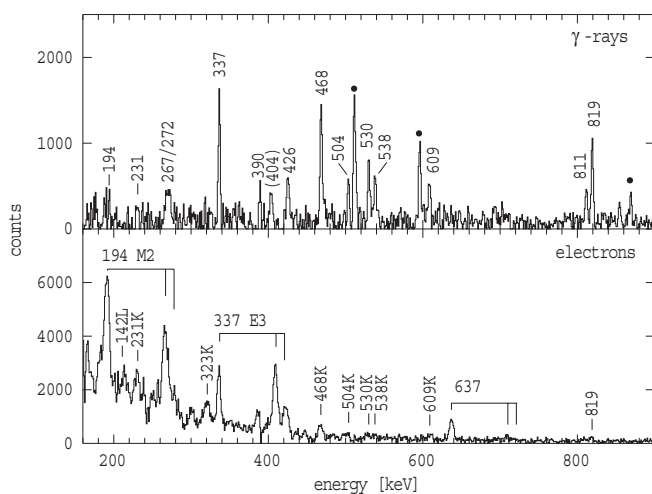

FIG. 1. Corresponding γ-ray and electron spectra recorded at the focal plane of the recoil spectrometer. Each spectrum is gated to select the 1–85 μs delayed time region, with the subsequent time period subtracted to remove activities. Contaminant γ rays that will not have associated electrons are indicated by filled circles.

TABLE I. Conversion coefficients in ^{189}Pb.

E_γ	Type	Experiment[a]	Assignment	Theory[b]				
				$E1$	$M1$	$E2$	$M2$	$E3$
194	K	5.3(11)	$M2$	0.0682	1.164	0.181	5.07	0.464
	L	<2.6(9)[c]		0.0121	0.200	0.220	1.47	3.09
	M	(<1.2)[d]		0.0028	0.0469	0.0576	0.370	0.850
	K/L	>2.0(8)		5.63	5.81	0.820	3.44	0.150
337	K	0.113(16)	$E3$	0.0186	0.254	0.0497	0.830	0.132
	L	0.181(26)		0.0031	0.0433	0.0246	0.196	0.194
	M	<0.086		0.0007	0.0101	0.0063	0.0481	0.0519
	K/L	0.62(12)		5.99	5.87	2.02	4.23	0.680
609	K	0.020(6)	($E3$)	0.0053	0.0527	0.0138	0.138	0.0332
468	K	0.023(3)	$E2$	0.0091	0.1054	0.0239	0.301	0.0606
530	K	0.021(4)	$E2$	0.0070	0.0759	0.0184	0.208	0.0454
538	K	0.018(3)	$E2$	0.0068	0.0730	0.0178	0.199	0.0439
637	K	0.41(16)	$E0 + M1 + E2$	0.00485	0.0469	0.0126	0.122	0.030
811	K	0.012(3)	$E2$	0.0031	0.0251	0.0079	0.0616	0.0177
819	K	0.008(2)	$E2$	0.0030	0.0245	0.0078	0.0601	0.0174

[a]For weak transitions, normalized delayed γ-ray intensities from Ref. [13] have been used.
[b]Reference [16].
[c]Contaminated by 267 and 272 K lines ($M1$ and $M1/E0$).
[d]Contaminated by the 279 K line ($M1/E0$).

should also be noted that the 194-keV transition could have a small $E3$ component, implying a somewhat lower total conversion.

Assignment of $J^\pi = 31/2^-$ to the 2435-keV state obviates the need to postulate an unobserved transition to explain its long-lived nature since the absolute probabilities for $E3$ and $M2$ decays are low. The corresponding transition strengths for decays from the isomer are listed in Table II. The 337-keV transition is an enhanced $E3$, whereas the 194- and 609-keV transitions are both relatively hindered. The configurations and implied configuration changes will be discussed in the following.

To establish the context, the systematics of the excitation energies of states associated with the lowest lying shears bands relative to the $13/2^+$ ($i_{13/2}$ neutron) intrinsic state are shown in Fig. 3, together with the newly assigned $31/2^-$ state in ^{189}Pb and the locus of excitation energies of the 11^- isomer in the neighboring even-even isotopes. It should be emphasized that in a number of cases, particularly ^{191}Pb and ^{193}Pb, the spins of the lowest state in each band are not firmly assigned and the excitation energy in ^{191}Pb could be higher by ∼30 keV because

of unobserved low-energy transitions. Furthermore, following the suggestion of Fotiades *et al.* [12], the spins assumed for the states in ^{193}Pb (shown as open symbols) are $1\hbar$ lower than the values currently adopted [6]. Nevertheless, the pattern is suggestive with the lowest state observed changing from $25/2^-$ in the heavier isotopes to $29/2^-$ in ^{191}Pb, with the present (unambiguously assigned) $31/2^-$ state in ^{189}Pb falling close to a smooth extrapolation from the heavier isotopes.

TABLE II. Transition strengths for decays from the $31/2^-$ 2435-keV isomeric state, with $\tau = 32^{+10}_{-2}$ μs [13].

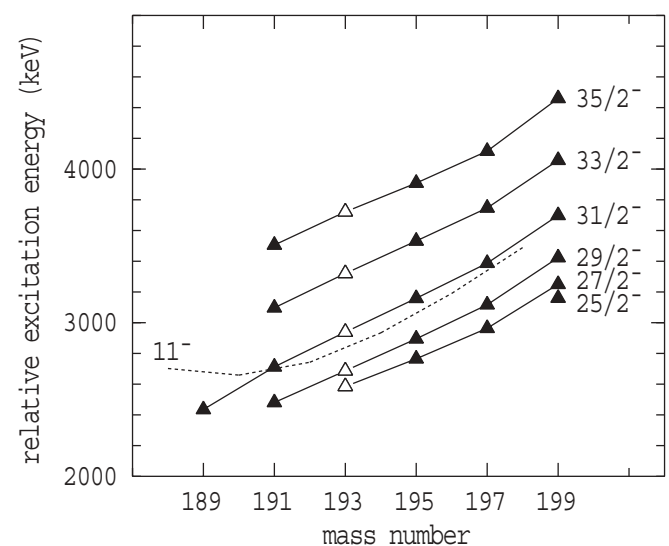| Final state J^π	E_γ (keV)	I_γ[a] relative	$\sigma\lambda$	α_T	Transition strength (W.u.)
$27/2^+$	194	22(5)	$M2$	7.03	$5.5^{+14}_{-22} \times 10^{-3}$
$25/2^+_2$	337	290(30)	$E3$	0.394	23.7^{+36}_{-81}
$25/2^-_1$	609	55(10)	$E3$	0.055	$7.2^{+15}_{-27} \times 10^{-2}$

[a]From Ref. [13].

FIG. 3. Energy systematics of proposed shears bands in the odd-A Pb isotopes, relative to the $13/2^+$ neutron-hole excitation. Note that the states in ^{193}Pb (open symbols) have been reduced by $1\hbar$ from those assigned (see text).

Although the observed energies will be related to the 11^- core excitation energy, it should be remembered that addition of a neutron affects the relative energies, in effect blocking the ground state compared to the even-even case. Moreover, the ground state in ^{188}Pb is significantly mixed because of shape coexistence [3] and hence will be depressed in energy by about 50 keV [3].

The change in the spin of the lowest state observed can be attributed to the effect of the residual interactions between the two-proton excitation and the seniority-one neutron hole, whose character changes as the $i_{13/2}$ neutron shell is depleted. To demonstrate this, a simplified calculation was carried out using the interactions known from two-particle multiplets in the Pb region.

These calculations follow the techniques of the empirical shell model (ESM) as described in our recent work [18]. The starting point is the set of two-particle residual interactions (see, e.g., Refs. [18–22]), although the present calculations are confined to a restricted case since the formalism is not appropriate for a system with a large number of holes. To show the general effects on the residual interactions as the neutron shell is depleted, the particle-particle interactions V_{pp} were obtained from the particle-hole interactions V_{ph} by using the Pandya transformation [19,23]. This requires, as input, the full set of interactions for any specific multiplet. All members of the $\pi h_{9/2} \nu i_{13/2}^{-1}$ multiplet, for example, are known from experiment and only a few of the $\pi i_{13/2} \nu i_{13/2}^{-1}$ multiplet are known empirically, but the remainder can be estimated, relatively reliably, from specific forces. It is possible then to generate an effective interaction V_{eff} as a function of the occupation probabilities and therefore the quasiparticle character of the $i_{13/2}$ neutron:
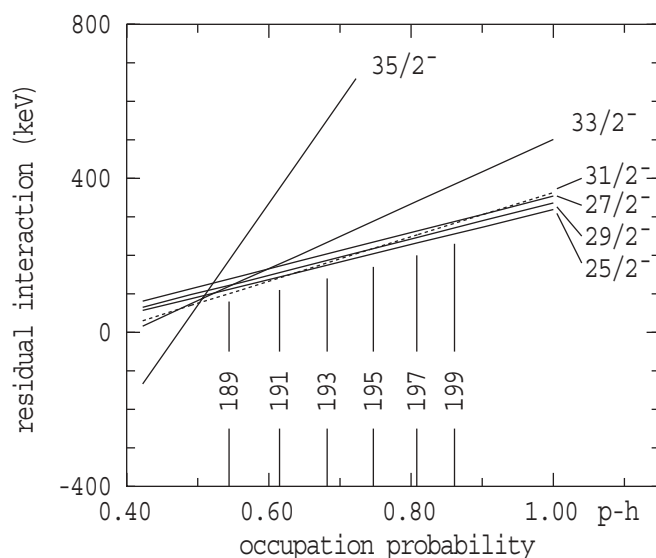
$$V_{eff} = U^2 V_{ph} + V^2 V_{pp}.$$

FIG. 4. Total residual interaction for the lowest states of the $\pi[h_{9/2}i_{13/2}]_{11^-} \otimes \nu i_{13/2}$ multiplet as a function of occupation probability.

This interaction can then be used together with the known proton-proton interactions to calculate the total residual interaction by recoupling the wave function into a sum of two-particle wave functions [24]. Selected results for the case where the proton component is restricted to $J^\pi = 11^-$ and coupled to the $i_{13/2}$ neutron, giving multiplets with $J^\pi = 9/2^-, 11/2^-, \ldots, 35/2^-$, are shown in Fig. 4 as a function of the particle-hole character of the $i_{13/2}$ neutron. The approximate position of each isotope with respect to the odd-neutron character is also shown schematically. Equivalent calculations were carried out for the $\pi[h_{9/2}^2]_{8^+} \otimes \nu i_{13/2}$ and $\pi[h_{9/2}f_{7/2}]_{8^+} \otimes \nu i_{13/2}$ configurations, leading to positive-parity states.

Although these calculations cannot be expected to give precise estimates given the simplifications and assumptions, the general trend from Fig. 4 is that in the upper part of the shell where the $i_{13/2}$ neutron is a hole, the repulsive interactive for mutually aligned protons and neutrons favors the intermediate spins, with $25/2^-$ being lowest, but with the $29/2^-$ state falling close by. The $[J_{max} - 2]$, $31/2^-$ coupling is not favored but it is predicted to fall to be the lowest member, approaching the middle of the shell (near ^{189}Pb). The $[J_{max} - 1]$ and J_{max} couplings give unfavored $33/2^-$ and $35/2^-$ states but these fall more rapidly and would be important (possibly leading to low-lying isomers) in ^{187}Pb. The equivalent calculations for coupling to the 8^+ two-proton excitation provide a consistent picture in that the $[J_{max} - 2]$, $25/2^+$ state drops in a similar fashion in moving toward the middle of the shell and would lie significantly below the $27/2^+$ member of the multiplet in ^{189}Pb, so that an $E3$ decay path from the $31/2^-$ state would be favored.

Of the observed transition strengths, the 337-keV $E3$ branch has an enhancement very similar to that observed for the $11^- \rightarrow 8^+$ transitions in the even-even isotopes in the range $^{190-196}$Pb [5]. As discussed in Ref. [4], given nominal configurations of $h_{9/2}i_{13/2}$ and $h_{9/2}^2$ for the 11^- and 8^+ two-proton states, the $11^- \rightarrow 8^+$ transition would correspond in principle to an orbital change of $\pi i_{13/2} \rightarrow \pi h_{9/2}$, a spin-flip transition for which an $E3$ strength of 3–5 W.u. is expected (a type-B transition in the categorization of Ref. [25]). A strength of ~20 W.u. would, in this region, normally be associated with a proton $i_{13/2} \rightarrow f_{7/2}$ configuration change, a stretched (or type-A) transition [25]. This apparent anomaly was interpreted [4] as a subtle effect of oblate deformation since deformation induces mixing of the $f_{7/2}$ configuration into the lowest $h_{9/2}$ proton orbitals present in the 8^+ configuration, resulting in more enhanced $E3$ transitions from the 11^- isomer.

The present observation of an enhanced $E3$ decay is indicative of related configurations (and deformations) in the $31/2^-$ isomer and the $25/2_2^+$ state to which it decays with a strength of about 24 W.u. In contrast the (energetically favored) 609-keV transition to the $25/2_1^+$ state is much weaker, being $\sim 7 \times 10^{-2}$ W.u., consistent with this state being a member of the seniority-three $\nu i_{13/2}^{-n}$ multiplet [13], a configuration that is very different from that of the $31/2^-$, 2435-keV state. (Note that in the previous work, the 2435-keV state had been assigned as a possible member of the $\nu i_{13/2}^{-n}$ multiplet with an unobserved low-energy transition feeding from the $33/2^+$ maximum spin member of the same multiplet, although this was somewhat at

odds with the energy systematics.) The 194-keV $M2$ branch to the 2241-keV state is also weak at about 5×10^{-3} W.u. A configuration for this state has not been proposed, although it could be the $[J_{\max} - 1]$ partner of the $[J_{\max} - 2]$, $25/2^+$ state at 2098 keV. The weak $M2$ branch could arise from both the change in coupling compared to the $31/2^-$ state and also the j-forbidden nature of a $\pi i_{13/2} \to \pi f_{7/2}$ transition. A $\pi i_{13/2} \to \pi h_{9/2}$ transition would, however, imply a larger $M2$, but not if a coupling change is involved.

The presence of an isomer and the main features of the isomeric decays can be interpreted therefore as the result of nonmaximal $(J_{\max} - 2)$ coupling of the $i_{13/2}$ neutron to the 11^- and 8^+ states of the core. The isomer is effectively a shears bandhead with protons and neutrons coupled at a relative angle of about $60°$.

In summary, direct conversion coefficient measurements in ^{189}Pb have resulted in an assignment of $J^\pi = 31/2^-$ to the 2435-keV state, and correspondingly to the identification

of that state as a long-lived isomer. The low-lying nature of this state and the change with respect to the heavier isotopes can be attributed to the change in character of the $i_{13/2}$ neutron, which becomes more particle-like toward the middle of the shell, thus moderating the repulsive proton-neutron interaction that dominates in the upper part of the shell.

[1] G. D. Dracoulis, A. P. Byrne, and A. M. Baxter, Phys. Lett. **B432**, 37 (1998).

[2] G. D. Dracoulis, A. P. Byrne, A. M. Baxter, P. M. Davidson, T. Kibédi, T. R. McGoram, R. A. Bark, and S. M. Mullins, Phys. Rev. C **60**, 014303 (1999).

[3] G. D. Dracoulis, G. J. Lane, A. P. Byrne, T. Kibédi, A. M. Baxter, A. O. Macchiavelli, P. Fallon, and R. M. Clark, Phys. Rev. C **69**, 054318 (2004).

[4] G. D. Dracoulis, T. Kibédi, A. P. Byrne, A. M. Baxter, S. M. Mullins, and R. A. Bark, Phys. Rev. C **63**, 061302(R) (2001).

[5] G. D. Dracoulis, G. J. Lane, T. M. Peaty, A. P. Byrne, A. M. Baxter, P. M. Davidson, A. N. Wilson, T. Kibédi, and F. R. Xu, Phys. Rev. C **72**, 064319 (2005).

[6] A. N. Andreyev *et al.*, Nature (London) **405**, 430 (2000).

[7] R. Julin, K. Helariutta, and M. Muikku, J. Phys. G: Nucl. Part. Phys. **27**, R109 (2001).

[8] H. Hübel, Prog. Part. Nucl. Phys. **54**, 1 (2005).

[9] R. M. Clark and A. O. Macchiavelli, Annu. Rev. Nucl. Part. Sci. **50**, 1 (2000).

[10] Amita, A. K. Jain, and B. Singh, At. Data Nucl. Data Tables **74**, 283 (2000).

[11] K. Vyvey *et al.*, Phys. Rev. Lett. **88**, 102502 (2002).

[12] N. Fotiades *et al.*, Phys. Rev. C **57**, 1624 (1998).

[13] A. M. Baxter *et al.*, Phys. Rev. C **71**, 054302 (2005).

[14] P. Nieminen, G. J. Lane, G. D. Dracoulis, T. Kibédi, M. Dasgupta, and D. J. Hinde, AIP Conf. Proc. **831**, 517 (2006).

[15] M. D. Rodríguez (to be published).

[16] T. Kibédi, T. W. Burrows, M. B. Trzhaskovskaya, P. M. Davidson, and C. J. Nestor Jr., Nucl. Instrum. Methods A **589**, 202 (2008).

[17] K. Van de Vel *et al.*, Phys. Rev. C **65**, 064301 (2002).

[18] G. D. Dracoulis, G. J. Lane, A. P. Byrne, P. M. Davidson, T. Kibédi, P. Nieminen, K. H. Maier, H. Watanabe, and A. N. Wilson, Phys. Rev. C **77**, 034308 (2008).

[19] J. P. Schiffer and W. W. True, Rev. Mod. Phys. **48**, 191 (1976).

[20] K. H. Maier *et al.*, Phys. Rev. C **76**, 064304 (2007).

[21] S. Bayer, A. P. Byrne, G. D. Dracoulis, A. M. Baxter, T. Kibédi, and F. G. Kondev, Nucl. Phys. **A694**, 3 (2001).

[22] A. R. Poletti, A. P. Byrne, G. D. Dracoulis, T. Kibédi, and P. M. Davidson, Nucl. Phys. **A756**, 83 (2005).

[23] S. P. Pandya, Phys. Rev. **103**, 956 (1956).

[24] P. M. Davidson, SESAME User Manual, Australian National University, Department of Nuclear Physics Internal Report P1636, 2005 (unpublished).

[25] I. Bergström and B. Fant, Phys. Scr. **31**, 26 (1985).